Contrib Mineral Petrol (1994) 117:241–252

Nigel B. W. Harris · Simon Kelley · Aral I. Okay

Post-collision magmatism and tectonics in northwest Anatolia

Received: 13 July 1993 / Accepted: 11 March 1994

Abstract A suite of biotite-hornblende granodiorite intrusions has been emplaced into blueschist-facies metasediments in northwest Anatolia, following collision between two continental margins, now represented by the Tavşanli and Sakarya zones. The $^{40}Ar/^{39}Ar$ ages of phengites and glaucophanes from the blueschists, metamorphosed under unusually high P-low T conditions ($P = 20 \pm 2$ kbar, $T = 430 \pm 30°$ C), suggest that metamorphism apparently occurred over a period spanning at least 20 Ma from 108 to 88 Ma. Post-tectonic granodiorites were emplaced during the Eocene (53 to 48 Ma) resulting in a cordierite and andalusite-bearing thermal aureole, indicative of pressures of ~ 3 kbar. Trace-element systematics of the granodiorites are consistent with a derivation either from mantle-derived magmas by fractional crystallisation in shallow magma chambers, or from anatexis of crustal lithologies of intermediate composition at pressures < 10 kbar. The preservation of high P-low T assemblages in the blueschists together with the range of ages determined for blueschist-facies metamorphism are indicative of rapid exhumation of delaminated fragments from a subducted continental margin. However decompression melting of the crust is unlikely to have been a significant cause of magmatism, both because exhumation of the blueschists from deep crustal levels predated magmatism by at least 25 Ma, and because of the small melt fraction (< 0.1) that may be generated in crustal lithologies by this process. Melting in the mantle wedge is required either to generate a primary melt for the derivation of magmas of intermediate composition or to provide an advective heat source for crustal melting. The cause of melt formation in the upper mantle may be related to the termination of subduction following collision during the Mid-Eocene.

N.B.W. Harris (✉) · S. Kelley
Department of Earth Sciences, Open University,
Milton Keynes MK7 6AA, UK

A.I. Okay
ITÜ, Maden Fakültesi, Jeoloji Bölümü, Ayazağa,
Istanbul, Turkey

Editorial responsibility: I. Parsons

Introduction

Fractional melting within the Earth's crust or mantle is a consequence of the solidus of the mineral assemblage being exceeded through an increase in temperature, a decrease in pressure or a change in the activities of volatile species. These variables can often be related to the prevailing tectonic environment as in volcanic arcs or rift zones. The causes of magmatism following continent-continent collision are however poorly understood, both because the major and trace elements from such melts are generally indistinguishable from those formed during active subduction (Pearce et al. 1984) and because a wide variety of mechanisms are potentially available for magmagenesis.

During the first few million years after subduction has ceased, magmas may continue to be generated in the mantle wedge. For example, calc-alkaline lavas were generated for at least 10 Ma after the end of subduction in the Basin-and-Range Province (Eaton 1982). Melting of pelitic lithologies occurs in the mid-crust a few tens of millions of years after collision, resulting from conductive heating within thickened crust combined with dissipative heating on active thrust zones (England et al. 1992). Advective heating from mantle-derived melts is a further cause of post-collision crustal melting (De Yoreo et al. 1989) and the relative contributions of conductive and advective heating in convergent orogens has been assessed by Sandiford et al. (1992). Uplift, either in response to isostatic forces on thickened crust or to wedge dynamics in the footwall of active thrusts, may result in decompression melting under vapour-absent conditions (Le Breton and Thompson 1988; Harris and

Massey 1994) thus providing a purely tectonic cause of post-collision magmatism. Finally, convective thinning of thickened lithosphere will result in rapid uplift (Houseman et al. 1981), causing melting of the upper mantle and generation of alkali basalts, as have been erupted across the Tibet Plateau about ~40 Ma after the initial continent-continent collision (Turner et al. 1993).

This paper documents the results of a study of post-collision Eocene granodiorites from northwest Anatolia that intrude and overprint blueschist-facies lithologies. The importance of this unusual association is that it represents an example of granitic magmatism formed within a collision zone where high *P*-low *T* assemblages are preserved, providing constraints on the thermal and tectonic evolution of the crust both during exhumation of high-pressure assemblages, and during magma emplacement. Hence it provides an ideal geological environment for an investigation into the relationship between magmatism and exhumation during post-collision tectonics.

Tectonic setting of northwest Anatolia

The blueschist-facies assemblages of northwest Anatolia are exposed within the Tavşanli Zone that formed the northern passive continental margin of the Tauride-Apulia plate during the Jurassic and Early Cretaceous, facing the Neo-Tethyan ocean (Okay 1984). This sequence was subducted by a north-dipping subduction zone beneath the Sakarya Zone, representing the Pontide continental margin (Okay 1984). The timing of collision between the two zones is poorly constrained. It is certainly earlier than Middle Eocene and probably after Turonian (89–50 Ma), and was predated by obduction of the ophiolite fragments now exposed along the collision zone (Fig. 1). The intervening Izmir-Ankara suture is presently marked by an active strike-slip fault that offsets Miocene conglomerates. Blueschist-facies metamorphism is a consequence of subduction of sedimentary lithologies, including phyllites, carbonates and intercalated cherts (Okay 1989), and has been dated as Upper Cretaceous (65–82 Ma) by K-Ar dating of phengites (Çoğulu and Krummenacher 1967), although glaucophane K-Ar ages as old as 125 Ma are cited in Okay (1986). Blueschist-facies metamorphism is believed to be broadly coeval with the timing of ophiolite obduction (Okay 1989) although there are no isotopic constraints on the obduction age. Uplift of the blueschists was probably a result of normal faulting along the blueschist/ophiolite interface.

North of the suture, Miocene leucogranites of crustal origin were emplaced into metasediments between 24 and 26 Ma ago, as exposed in the Uludağ Massif (Bingöl et al. 1982). South of the suture, four post-tectonic biotite-hornblende granodiorites are emplaced into blueschist-facies assemblages and overlying ophiolitic fragments (Fig. 1), but of these only the Topuk and Orhaneli bodies are well exposed. Published K-Ar ages for the Topuk intrusion range from 43–64 Ma (Bingöl et al. 1982) compared with biotite-whole rock Rb-Sr ages of 49–52 Ma (Ataman 1972). For the Orhaneli granodiorite, biotite-whole rock Rb-Sr ages vary from 63 Ma (Vachette et al. 1968) to 49–52 Ma (Ataman 1972), somewhat older than the ages obtained from the easterly, poorly exposed, Gürgenyayla granodiorite (44–46 Ma; Ataman 1973).

Field relations of the intrusives

The Orhaneli intrusion forms a sub-circular body, 15 km in diameter, emplaced 30 km south of the suture. The pluton is a homogeneous, medium-grained granodiorite, which has intruded a blueschist-facies regional metamorphic sequence of quartz-mica schist, graphitic mica schist, metaquartzite, and minor metabasite overlain by marble. The metabasites are characterised by sodic amphibole + lawsonite and sodic amphibole + jadeite + paragonite + quartz parageneses (Okay and Kelly 1994). Blueschist-facies assemblages have re-equilibrated within a one-kilometre wide aureole surrounding the granodiorite in response to thermal metamorphism. Along its western margin the granodiorite is unconformably overlain by Miocene dacite flows and acid tuffs. A thin (2 m) basal conglomerate indicates a significant period of exposure during the Miocene, prior to eruption of the volcanics.

The fabric of the granodiorite is generally isotropic with a local foliation along its south-eastern margin, defined by planar alignments of plagioclase, amphibole and biotite. The emplacement of the near-circular pluton with a marginal foliation is probably the consequence of syn-emplacement ballooning around the margin of a diapiric intrusion. Forceful intrusion has resulted in asymmetric folds around its margin, together with the development of a marginal syncline along its northern contact. Contacts are locally concordant, with screens and xenoliths of country rock alternating with intrusive facies over a distance of 500 m. The contact aureole along the eastern contact of the granodiorite with marble and mica schist is marked by the development of diopside-rich skarns in the calc-silicates and the growth of biotite at the expense of phengite in the metapelites. At one locality, porphyroblasts of andalusite and cordierite have been recognised. Andalusite, together with sillimanite, has also been reported in the aureole of the Topuk granodiorite to the north (Lisenbee 1972).

The equigranular granodiorite is made up of plagioclase (50–60%, by volume), quartz (20–25%), biotite (10–15%), alkali feldspar (~ 10%), and hornblende (~ 5%). Plagioclase is euhedral andesine, often with oscillatory zoning between An_{33} and An_{50}. Alkali feldspar is untwinned with some perthitic exsolution, and is clearly a late phase to crystallise since it is both allotriomorphic and contains inclusions of plagioclase and hornblende. Ilmenite and sphene are common accessories. Geochemical sampling has been restricted to fresh exposures since many outcrops are weathered with secondary chlorite, muscovite and epidote growth.

The granodiorite is generally homogeneous at its present level of exposure apart from the northern margin where a leucocratic aplitic granite is exposed, characterised by perthite, and quartz, with minor plagioclase and hornblende and accessory sphene. There is a gradational transition from the granodiorite and the aplitic carapace over a distance of ~5 m.

Within the granodiorite small (< 300 mm) spherical quartz dioritic enclaves, finer grained than the host granodiorite, contain megacrysts of amphibole and plagioclase in an amphibole, biotite, plagioclase and quartz matrix. These have become strongly ellipsoidal around the margins of the granodiorite where a penetrative fabric is preserved. The origin of the enclaves is equivocal, but their fine grain size coupled with their ductile response to deformation along the margins of the intrusion suggests that they represent chilled globules of dioritic magma, that were locally deformed whilst still in a plastic state. The megacrysts are similar in composition and habit to phases within the granodiorite and presumably grew during the early crystallisation history of the granodiorite. Such enclaves may be the results of a period of dioritic magmatism that immediately pre-dates the granodiorite intrusion, coeval with hornblende-augite diorite dykes, that are cut by the Topuk granodiorite to the north (Lisenbee 1972).

The Topuk granodiorite is an elliptical pluton, 12 × 15 km, locally sheared by a post-emplacement east–west fabric parallel to its long axis and to the suture. Its core is intruded by microgranodiorite, which probably represents a dyke parallel to the contact of the roof zone (Lisenbee 1972). In other respects, its mineralogy and mineral fabric are indistinguishable from those of the Orhaneli intrusion.

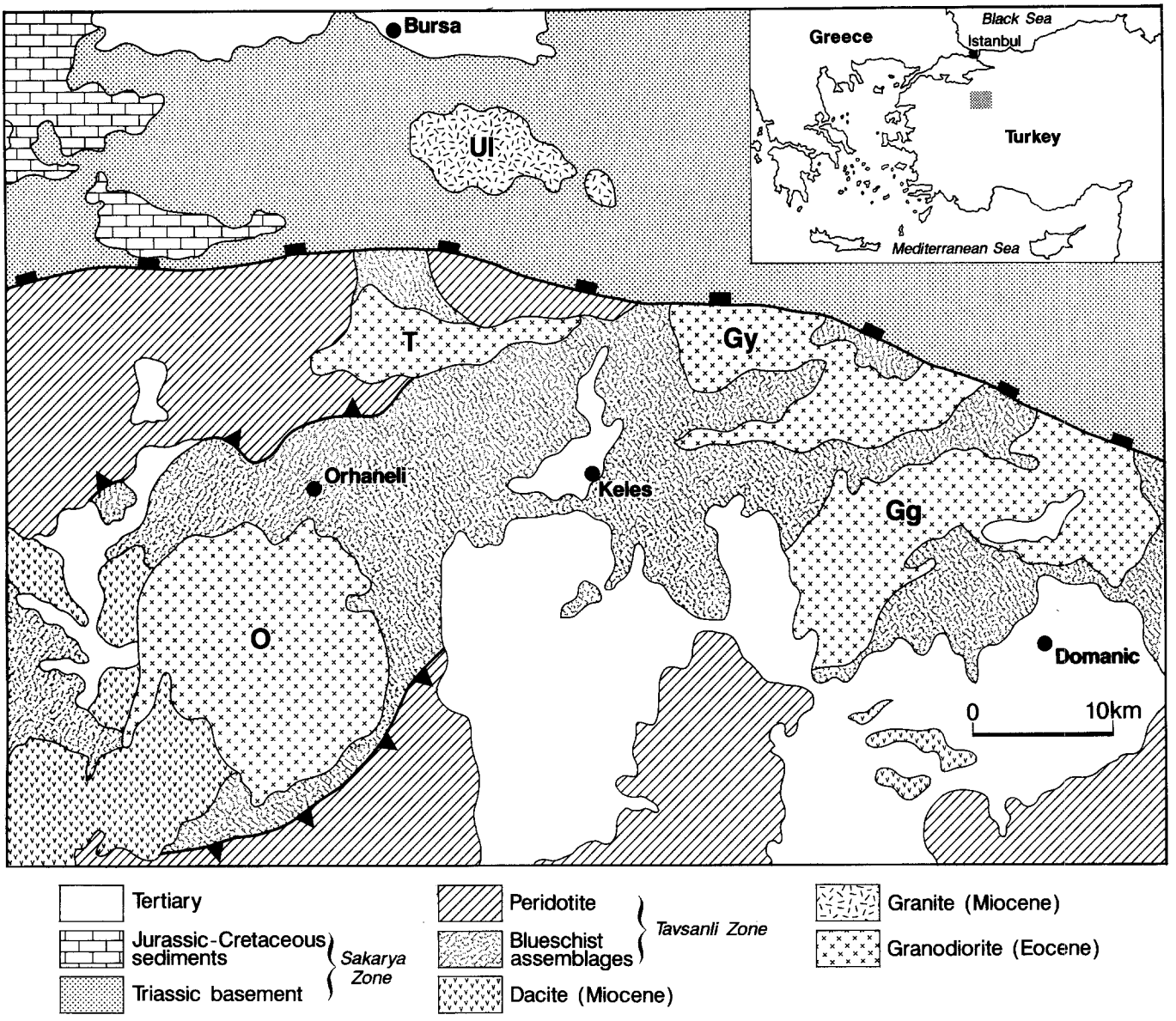

Fig. 1 Geological map of the Orhaneli region of western Turkey. (*O* Orhaneli, *T* Topuk, *Gy* Göynükbelen, *Gg* Gürgenyayla granodiorites, *Ul* Uludağ granite)

Analytical techniques

Mineral analyses were undertaken on an SX-50 Cameca electron microprobe in the Department of Earth Sciences, University of Cambridge. The accelerating voltage was 20 kV, beam current 10 nA and beam size 10 μm.

Whole rock chemical analyses were made on an ARL 8420 + dual goniometer wavelength dispersive XRF spectrometer at the Department of Earth Sciences, Open University. Major elements were determined from fused glass discs and trace elements (Rb, Sr, Ba, Nb, Zr, Y) from pressed powder pellets. Rare earth elements and Ta, Hf, Th, U were analysed by instrumental neutron activation analysis at the Open University and computed using the method of Potts et al. (1981).

For Ar isotope analyses, polished slices (10 mm × 10 mm × 1 mm) were ultrasonically cleaned in methanol, wrapped in foil and irradiated by 10^{18} neutrons cm^{-2} at the Ford Reactor, Michigan, monitored by hornblende standard mmhb1 (Age = 520.4 Ma, Samson and Alexander 1987). Argon was extracted from small areas by 10–100 ms laser pulses generated by a computer controlled external shutter and a Spectron SL902 CW Nd-YAG laser producing up to 17 W TEM_{00}. Gases released were analysed by a MAP 215-50 noble-gas mass spectrometer. Data were corrected for discrimination and blanks by the procedure outlined in Hawkesworth et al. (1992), using correction factors $(^{39}Ar/^{37}Ar)_{Ca} = 0.00078$; $(^{36}Ar/^{37}Ar)_{Ca} = 0.00021$; $(^{40}Ar/^{39}Ar)_{K} = 0.031$ based upon analysis of calcium and potassium salts.

Mineral chemistry and thermobarometry

Regional blueschist metamorphism

Mineral assemblages from blueschist metaclastics exposed in the Kocasu region, 10 kilometres west of the Orhaneli granodiorite, have been the subject of a detailed thermobarometric study (Okay and Kelley 1994).

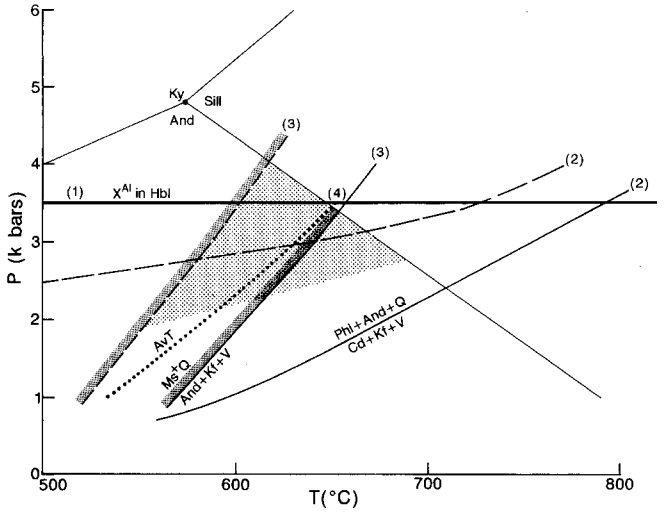

Fig. 2 Pressure-temperature constraints from phase equilibria derived from thermal aureole of Orhaneli granodiorite. (*1*) Al in hornblende (Schmidt 1992); (*2*) Phl + And + Q = Cd + Kf + V; (*3*) Ms + Q = And + Kf + V; (*4*) average temperature assuming $a_{H_2O} = 0.5$. All thermodynamic data (except for *1*) from Holland and Powell (1985, 1990). *Shaded area* indicates preferred *P-T* field for aureole assuming $a_{H_2O} = 0.5$. (*Hbl* hornblende, *Ky* kyanite, *And* andalusite, *Q* quartz, *Phl* phlogopite, *Cd* cordierite, *Kf* alkali feldspar, *Ms* muscovite, *V* vapour). For equilibria (*2*) and (3), *dashed lines* indicate $a_{H_2O} = 0.5$, *solid lines* $a_{H_2O} = 1$

The jadeite + paragonite + quartz assemblage constrains the pressure to between 12 and 25 kbar, and the silica content of the phengites gives a minimum pressure of 14 kbars at 430° C (Massone and Schreyer 1987). Pressures are further constrained by the equilibria involving chloritoid, glaucophane, paragonite, chlorite and quartz to 20 ± 2 kbar at 430° C, derived from the programme THERMOCALC and the enlarged self-consistent thermodynamic dataset of Holland and Powell (1990). The absence of garnet in both metabasic and metapelitic compositions indicates maximum temperatures of about 450° C, while the chloritoid-glaucophane equilibria indicate minimum temperatures of 420° C at 20 kbar. The overall estimate for the *P-T* conditions of metamorphism is 430 ± 30° C and 20 ± 2 kbar for the Kocasu region (Okay and Kelley 1994). The blueschist sequence in this region can be traced laterally to the western margin of the granodiorite indicating similar *P-T* conditions for the blueschists surrounding the granodiorite.

Depth of intrusion of granodiorite

Conditions of emplacement for the granodiorite can be determined by hornblende-plagioclase thermometry (Blundy and Holland 1990) which yields temperatures of 720–770 (± 75° C), with lower temperatures recorded by the rims of zoned plagioclase crystals. The peak temperature provides a minimum constraint on the liquidus temperature and is consistent with experimentally determined crystallisation temperatures for intermediate magmas (Piwinskii 1973). Emplacement may have been at somewhat lower temperatures if a crytal-magma mix was intruded.

An approximate pressure of emplacement is provided by the Al content of amphibole. Pressures of 3.4 ± 2.0 kbar are derived from the formulation of Hammarstrom and Zen (1986) and a more recent and precise barometer (Schmidt 1992) yields 3.5 ± 0.6 kbar (Fig. 2).

Assemblages from pelites within the thermal aureole include andalusite-cordierite-alkali feldspar-plagioclase-quartz-biotite. The presence of andalusite in the absence of muscovite indicates that conditions have exceeded those required for muscovite breakdown in the andalusite stability field which provides a maximum pressure constraint of 3.5 kbar (for $a_{H_2O} = 1$) which increases to 4 kbar (for $a_{H_2O} = 0.5$). The best-constrained equilibrium in the aureole assemblage is given by

Andalusite + Phlogopite + Quartz =
Cordierite + Alkali Feldspar + H_2O.

This provides a barometer that is strongly dependant on water activity. If $a_{H_2O} = 1.0$, a maximum pressure of 2.4 ± 0.8 kbar is obtained from activities calculated from mineral compositions in Table 1, based on the enlarged self-consistent thermodynamic dataset of Holland and Powell (1990). This rises to a pressure of 3.2 ± 0.8 kbar for $a_{H_2O} = 0.5$ (Fig. 2).

There is no independent evidence for water activity during intrusion of the granodiorite, but the statistical analysis of multiple equilibria provided by coexisting phases as given by Powell and Holland (1985) suggests that a high water activity requires a low pressure of emplacement. If $a_{H_2O} = 1$ then the available thermometers from the coexisting endmembers quartz, Mg-cordierite, Fe-cordierite, phlogopite, annite, eastonite, alkali feldspar and andalusite only provide a statistical fit within 95% confidence limits for pressure < 1 kbar. The calculated temperature at this pressure is 537 ± 30° C. At lower water activities, this constraint is relaxed; for $a_{H_2O} = 0.5$, the data fit up to pressures of ~ 3.5 kbar giving temperatures of 655 ± 35° C. Hence barometry from phase equilibria in the aureole and from Al concentrations in amphibole from the igneous assemblage can be reconciled at pressures of 3.0–3.5 kbar provided $a_{H_2O} < 1$. Temperatures recorded by geothermometers within the aureole are only of local significance since lateral temperature gradients away from the margin of the intrusion will be steep. The presence of sillimanite within some aureole assemblages from the Topuk intrusion (Lisenbee 1972) indicates higher temperatures were reached locally in the aureole.

We conclude that the Orhaneli intrusion was emplaced at pressures of 3 ± 1 kbar (~ 10km) and that water activities, at least locally within the aureole, were less than unity. Temperatures in the analysed assemblage from the aureole did not exceed 690° C, although magmatic temperatures were in excess of 770°C.

Table 1 Representative mineral analyses from Orhaneli intrusion and country rock (*Pl* plagioclase, *Hbl* hornblende, *Bt* biotite, *Cd* cordierite, *c* core, *r* rim)

Sample	Orhaneli granodiorite				Thermal aureole	
	Pl (c)	Pl (r)	Hbl	Bt	Cd	Bt
	3861	3861	3861	3861	3867a	3867a
Wt%						
SiO_2	57.81	59.33	45.74	36.08	47.39	34.36
TiO_2	0.01	0.00	0.92	3.51	0.02	2.85
Al_2O_3	25.87	25.05	7.83	14.49	32.53	19.95
Fe_2O_3	0.19	0.10	4.20	–	1.66	–
FeO	–	–	11.44	17.84	10.18	22.56
MnO	0.00	0.00	0.70	0.73	0.53	0.11
MgO	0.00	0.00	12.30	12.22	6.11	6.28
CaO	7.34	6.55	12.06	0.00	0.05	0.00
Na_2O	7.12	8.04	1.17	0.07	0.14	0.00
K_2O	0.33	0.18	0.74	9.57	0.01	9.45
Total	98.67	99.25	97.10	94.51	98.62	95.56
O	8	8	23	11	18	11
Si	2.62	2.67	6.81	2.78	4.95	2.65
Ti	0.00	0.00	0.10	0.20	0.00	0.17
Al	1.38	1.33	1.38	1.31	4.00	1.81
Fe^{3+}	0.07	0.03	0.47	–	0.13	–
Fe^{2+}	–	–	1.43	1.15	0.89	1.45
Mn	0.00	0.00	0.09	0.05	0.05	0.01
Mg	0.00	0.32	2.73	1.40	0.95	0.72
Ca	0.36	0.70	1.93	0.00	0.01	0.00
Na	0.63	0.01	0.34	0.01	0.03	0.00
K	0.02	8.04	0.14	0.94	0.00	0.93

Geochemistry of the Orhaneli and Topuk intrusions

Major-element geochemistry of the Orhaneli granodiorite indicates a uniform metaluminous, calc-alkaline composition with silica contents of 63–65% (Table 2). The Topuk granodiorite includes somewhat higher silica contents (65–69%) but in other respects is geochemically similar to both the Orhaneli granodiorite and to the Gürgenyala and Göynükbelen granodiorites intruded south of the Izmir-Ankara suture (Ercan and Türkecan 1984). The aplitic samples from the Orhaneli carapace are characterised by the major element chemistry of a peraluminous rhyolite (SiO_2 = 70–72%), lower Ca, Fe and Mg and higher Na and K compared to the granodiorite. These trends are consistent with formation of the aplitic rhyolite by fractionation of amphibole and possibly plagioclase from the granodioritic magma.

The trace-element geochemical trends from both granodiorites show enrichment in LIL (large-ion-lithophile) elements (Fig. 3a) with depletion of HFS (high-field-strength) elements such as Zr, Hf and HREE (heavy-rare-earth elements) relative to an Ocean Ridge Granite (Pearce et al. 1984) similar to both volcanic-arc and post-collision intrusions. The Topuk granodiorite is slightly enriched in Y and HREE but depleted in Ba, Sr and Th, relative to the Orhaneli samples. No differences were found in trace-element geochemistry between the fine-grained and the medium-grained facies within the Topuk intrusion, indicating a common source.

The aplitic facies from the Orhaneli pluton demonstrates variable trace-element characteristics compared to the granodiorite. The LILE (Rb, Ba and Th) are strongly enriched whereas Y is depleted. Incompatible trace-element ratios, such as Nb/Ta, are unusually high (> 30) for magmatic rocks, reflecting the relative stability of HFSE-volatile complexes rather than crystal/liquid equilibrium.

The absence of a detectable europium anomaly in the chondrite-normalised REE plot for the Orhaneli granodiorite (Fig. 4a) suggests that plagioclase fractionation has not played a significant role its formation. In contrast, the negative Eu anomaly observed in some samples from the Topuk intrusion (Fig. 4a) indicates the equilibration of the melt with feldspar. The HREE and Y depletion may be controlled by garnet in the source, fractionation of amphibole or accessory phase behaviour which may become increasingly important in more evolved melts. For the granodiorites, the lack of correlation between HREE (or Y) and Zr abundances suggests that zircon fractionation has not contributed significantly to REE evolution in the magma.

For the aplitic facies, Y and HREE-depletion (Fig. 3a) probably resulted from fractionation of amphibole, consistent with the shift from metaluminous to peraluminous compositions. However, petrogenetic modelling for aplitic rocks is poorly constrained due to the uncertainties in crystal/liquid distribution coefficients during volatile-rich fractionation. The highly variable LILE abundances reflect the stability of accessory phases under conditions of variable fluid flux during the final stages of crystallization.

Available data can not confirm whether the quartz-diorite enclaves were cosanguineous with the granodiorite because subsolidus feldspar growth has clearly occurred within the enclaves, thus modifying the initial igneous composition, at least for LIL elements. It could be argued that the depletion in Ba and Y seen in the host granodiorite relative to the enclaves indicates that a combination of amphibole and biotite fractionation has controlled magma evolution.

Ar-Ar chronology

Laser-spot analyses were performed on biotite, hornblende and glaucophane from the Orhaneli and Topuk granodiorites, a hornfels from the margin of the Orhaneli intrusion, two blueschists and a garnet amphibolite at the base of the ophiolite sequence. Analyses from between 5 and 10 laser spots were plotted on a $^{36}Ar/^{40}Ar$ versus $^{39}Ar/^{40}Ar$ diagram for each sample to determine both the age and $^{36}Ar/^{40}Ar$ intercept value (Fig. 5, Table 3).

Ten laser-spot analyses of biotite from the Orhaneli granodiorite (4419a) yielded a good isochron with an

Table 2 Chemical analyses from Orhaneli and Topuk intrusions (*LOI* loss on ignition)

Sample	Orhaneli granodiorite			Topuk granodiorite				Enclaves		Aplite	
	3992	4219	3905	3861	4425A	4427A	4429A	4413A	4419B	3900	3897
Wt%											
SiO_2	63.65	64.75	65.16	65.44	65.86	69.26	65.51	55.26	54.11	69.53	72.25
TiO_2	0.44	0.45	0.39	0.40	0.40	0.31	0.41	0.69	0.74	0.17	0.22
Al_2O_3	17.27	16.66	16.67	16.88	16.65	16.08	16.82	16.34	18.48	15.65	14.91
Fe_2O_3[a]	4.37	4.40	3.76	3.64	4.39	3.37	4.48	7.65	8.05	1.69	0.81
MnO	0.10	0.09	0.09	0.08	0.11	0.11	0.14	0.32	0.24	0.01	0.01
MgO	1.77	1.91	1.48	1.46	1.76	1.06	1.26	5.78	4.49	0.17	0.08
CaO	5.27	4.93	4.96	4.77	5.28	4.41	5.27	7.83	7.25	0.51	0.15
Na_2O	3.92	3.55	3.99	3.86	3.29	3.65	3.62	2.86	3.83	5.96	4.81
K_2O	2.05	2.27	1.72	2.16	1.92	1.99	1.91	2.03	1.92	4.95	6.08
P_2O_5	0.23	0.13	0.12	0.19	0.14	0.11	0.14	0.26	0.14	0.04	0.06
LOI	0.50	0.68	0.71	0.57	0.91	0.49	0.63	1.22	0.99	0.37	0.47
Total	99.57	99.82	99.05	99.45	100.71	100.84	100.19	100.23	100.25	99.05	99.84
Ppm											
Rb	73	71	62	76	64	70	72	78	77	167	136
Ba	848	672	535	672	343	467	402	634	483	1299	1266
Sr	714	380	477	550	291	292	329	366	335	926	547
Nb	10	8	9	10	7	8	9	11	14	18	21
Zr	175	99	107	129	113	122	141	64	102	256	103
Y	19	17	17	17	23	21	25	44	45	11	
Ta	0.54	0.53	0.65	0.66	1.00	0.59	0.56	0.35	0.64	0.58	0.62
Hf	4.34	2.94	3.35	3.97	3.39	3.53	3.98	2.45	3.28	8.98	3.16
Th	12.10	8.04	9.19	9.42	6.15	9.56	8.94	4.46	9.09	76.10	12.40
U	2.21	2.92	2.93	1.39	4.29	1.87	2.11	1.30	2.36	15.70	3.98
La	42.60	16.20	23.60	25.60	19.40	25.40	27.60	15.10	26.40	47.40	34.00
Ce	81.70	32.60	44.20	51.00	46.60	49.50	54.50	39.50	46.30	83.30	80.50
Nd	33.80	16.10	18.20	24.40	30.00	21.30	23.80	33.70	20.80	30.70	33.10
Sm	5.13	2.96	3.43	4.10	6.80	3.69	4.31	7.87	3.81	4.25	4.32
Eu	1.38	0.88	0.88	1.12	1.58	0.97	1.07	1.91	0.96	1.22	0.99
Tb	0.59	0.44	0.49	0.52	1.19	0.56	0.67	1.22	0.57	0.47	0.40
Yb	1.89	1.80	1.88	1.87	4.65	2.32	2.69	4.52	2.65	0.82	0.66
Lu	0.28	0.29	0.31	0.32	0.77	0.38	0.46	0.76	0.47	0.12	0.09

[a] All Fe calculated as Fe_2O_3

age of 52.6 ± 0.4 Ma and an MSWD of 1.6 (Fig. 5a). The non-radiogenic component falls within errors of the atmospheric ratio ($^{40}Ar/^{36}Ar = 302 \pm 8$). Five analyses of fine-grained biotite (with minor amphibole intergrowth) from a hornfels (4410), sampled two metres from the granodiorite contact, yield an isochron age of 52.4 ± 1.4 Ma with an MSWD of 0.5 (Fig. 5b) and an intercept of 301 ± 10. Since ages from both granodiorite and its fine-grained hornfels are within error, they indicate rapid cooling after intrusion at a high level in the crust, 52.6 ± 0.4 Ma ago.

Laser-spot ages of six biotite and two hornblende grains from the Topuk granodiorite (4427a) yielded an isochron of 47.8 ± 0.4 Ma with an MSWD of 1.4 (Fig. 5c) and an intercept indicating small amounts of excess argon ($^{40}Ar/^{36}Ar = 314 \pm 5$) possibly reflecting argon introduced during the deformation of this pluton which has undergone significant ductile/brittle deformation. The hornblende analyses do not yield a significantly different age when separated from the biotite, though the lower potassium content makes the ages less precise. The age of the Topuk granodiorite is therefore younger than that of the Orhaneli intrusion, though the ages differ by less than 4 Ma.

Two blueschist samples were analysed from the same locality; a glaucophane-lawsonite metachert (4414a), and glaucophane-albite-clinozoisite metabasite (4414b). Phengite was not detected in either sample. Seven laser-spot analyses of large (1–2 mm in length) glaucophanes in sample 4414a yielded an isochron age of 108.1 ± 3.7 Ma and an MSWD of 1.2 (Fig. 5d). However, this sample has a significant excess argon component reflected in the intercept value of 486 ± 11 and all analyses released greater than 50% non-radiogenic argon. The low MSWD of the isochron reflects the homogeneity of the excess argon component in the glaucophanes, implying that the age is real. The age falls within the range of K-Ar ages (125–65 Ma) from the blueschists of the Tavşanli Zone (Okay 1986) as does a laser $^{40}Ar/^{39}Ar$ analysis of phengite from a blueschist 15 km further west that yielded an age of 88 ± 1 Ma (Okay and Kelley 1994). Sample

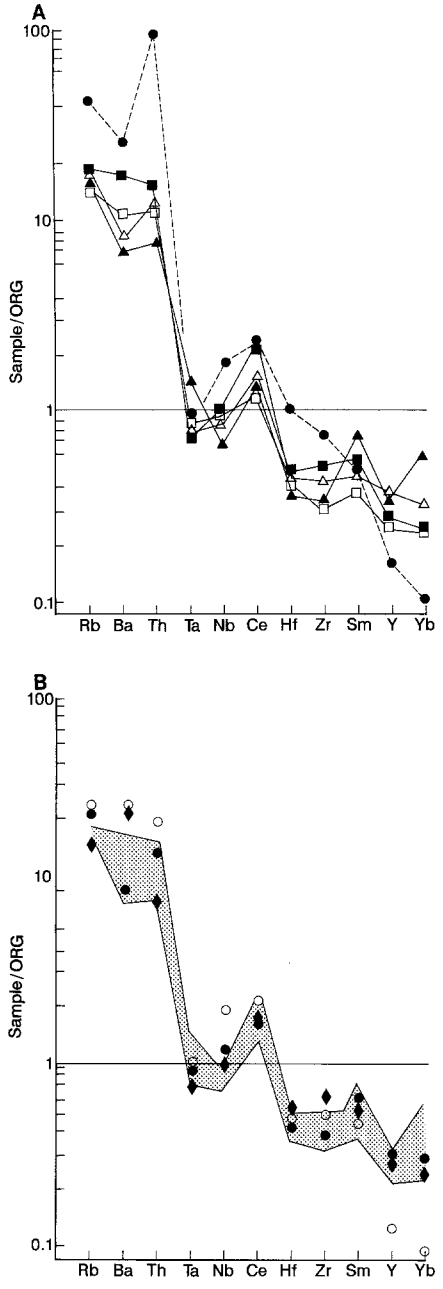

Fig. 3A,B Trace-element variation diagram, normalised against ORG (Pearce et al. 1984). **A** Orhaneli granodiorite (■ 3992, □ 3905), Topuk granodiorite (▲ 4425a, △ 4429a), Orhaneli aplite (● 3900). **B** (● Quartz diorite from Adamello Massif, $SiO_2 = 65.2\%$, Dupuy et al. 1982, ○ Granodiorite from Idaho, $SiO_2 = 71.3\%$, Clarke 1990, ◆ Dacite from Basin-and Range, $SiO_2 = 63.1\%$, Davis et al. 1993). *Shaded area* indicates range from Orhaneli and Topuk granodiorites

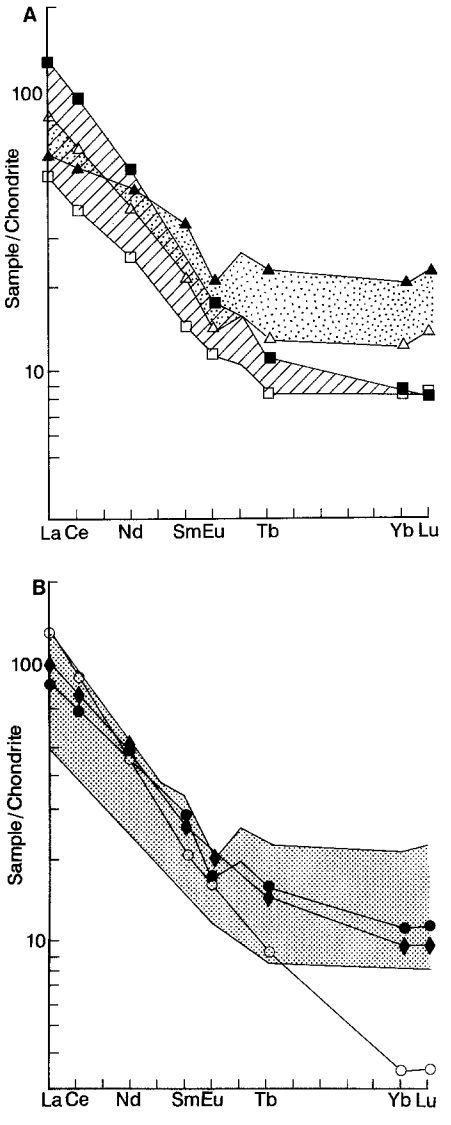

Fig. 4A,B Chondrite-normalised rare-earth element diagram. **A** Orhaneli granodiorite *diagonal shading* (■ 3992, □ 3905), Topuk granodiorite *stipple* (▲ 4425a, △ 4429a) **B** (● Quartz diorite from Adamello Massif, $SiO_2 = 65.2\%$, Dupuy et al. 1982, ○ Granodiorite from Idaho, $SiO_2 = 71.3\%$, Clarke 1990, ◆ Dacite from New Mexico, Basin-and Range Province, $SiO_2 = 63.1\%$, Davis et al. 1993). *Shaded area* indicates range from Orhaneli and Topuk granodiorites

4414b did not help constrain the chronology of blueschist metamorphism, though it exhibited a similar excess argon component to 4414a (Fig. 5d). The greater spread in $^{36}Ar/^{40}Ar$ ratios from 4414b probably reflects later alteration and carbonate filled microfractures observed in the section.

Although no laboratory derived argon diffusion data exists for glaucophane, where it has been measured glaucophane has generally yielded concordant or younger ages than coexisting white micas (McDowell et al. 1984 and references therein). The reason for the apparent variation of closure temperatures probably lies in the inclusion of small quantities of fine-grained impurities such as white mica, which have a marked effect upon ages of this low potassium mineral (Sisson and Onstott 1986). The reversed situation in the Tavşanli Zone may reflect true variation of the ages of peak metamorphism in the blueschists. Moreover pristine blueschist-facies assemblages were selected so that

Table 3 Ar-isotope results and isochron ages (*Gd* granodiorite, *Hfl* hornfels, *Gt* garnet, *Bt* biotite, *Gl* glaucophane, *Hbl* hornblende)

Sample	Lithology	Mineral	$^{40}Ar^*/^{39}Ar$	$^{40}Ar/^{36}Ar$	MSWD	*n*	Age (Ma)
4419a	Gd (Orhaneli)	Bt	5.409 ± 0.148	301 ± 10	1.6	10	52.4 ± 1.4
4410	Hfl (Orhaneli)	Bt	5.433 ± 0.039	302 ± 8	0.5	5	52.6 ± 0.4
4427a	Gd (Topuk)	Bt + Hbl	4.927 ± 0.038	314 ± 5	1.4	8	47.8 ± 0.4
4414a	Blueschist	Gl	11.328 ± 0.396	486 ± 11	1.2	7	108.1 ± 3.7
4433	Blueschist	Gl	2.538 ± 0.028	–	–	9	–
4415b	Gt-amphibolite	Hbl	10.584 ± 0.401	292 ± 15	0.9	9	101.1 ± 3.8

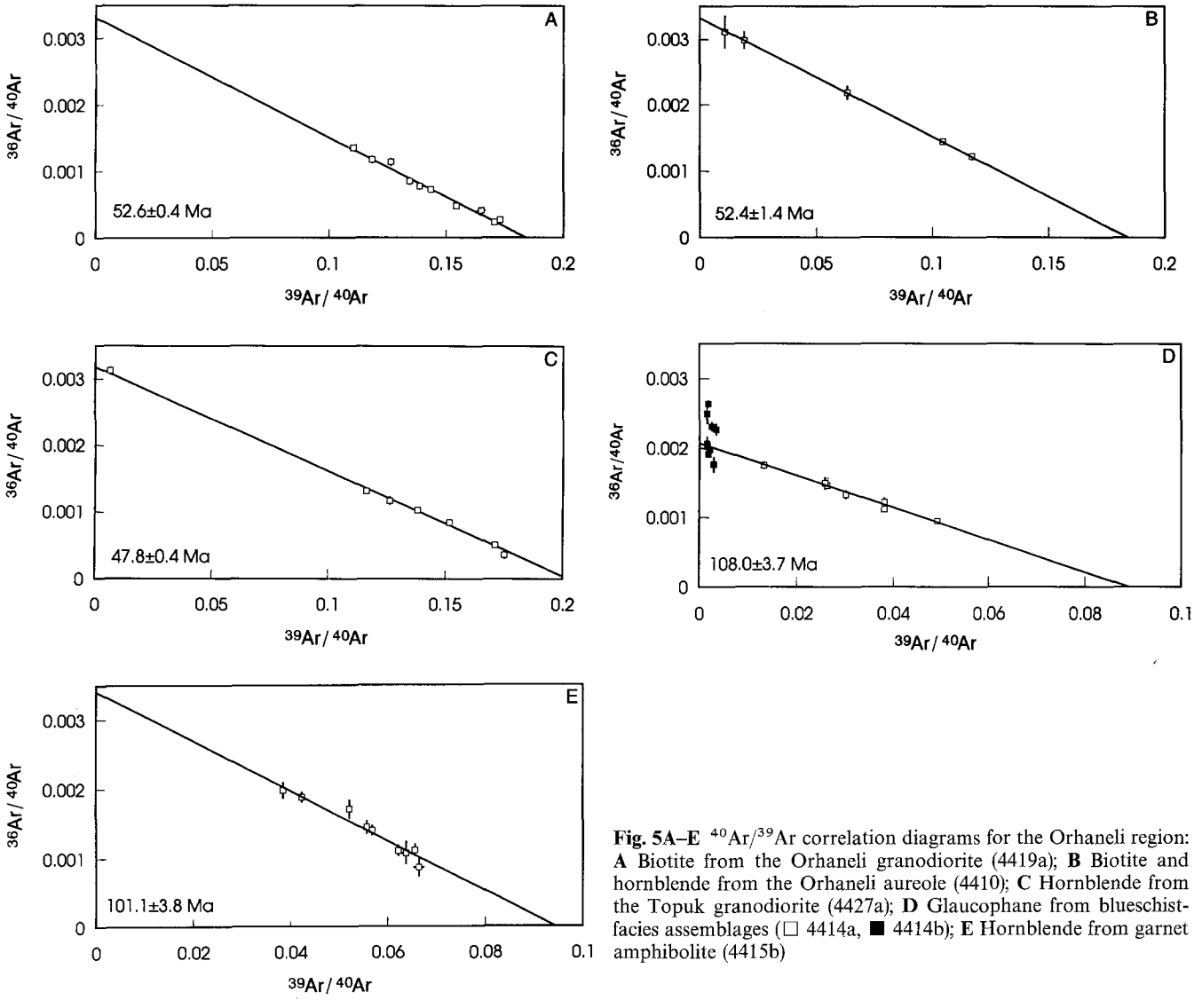

Fig. 5A–E $^{40}Ar/^{39}Ar$ correlation diagrams for the Orhaneli region: **A** Biotite from the Orhaneli granodiorite (4419a); **B** Biotite and hornblende from the Orhaneli aureole (4410); **C** Hornblende from the Topuk granodiorite (4427a); **D** Glaucophane from blueschist-facies assemblages (□ 4414a, ■ 4414b); **E** Hornblende from garnet amphibolite (4415b)

there is no petrographic evidence to support resetting of ages during a greenschist overprint. Further work is underway to resolve the significance of the range in ages for blueschist metamorphism.

The garnet amphibolite (4415b) was sampled from a thrust-bound pod beneath the ophiolite sequence. Nine laser-spot analyses of amphibole yielded an isochron age of 101.1 ± 3.8 Ma with an MSWD of 0.9. The intercept value lies within errors of atmospheric argon ($^{40}Ar/^{36}Ar = 292 \pm 15$). This provides an age for early cooling from amphibolite-grade metamorphism of the metamorphic sole of the obducted ophiolite.

Petrogenesis of the granodiorites

The Orhaneli and Topuk intrusions are part of a suite of Eocene diorites and granodiorites from northwest Anatolia that post-date collision. The absence of

compositions more primitive than quartz diorite suggests either that basic magmas have differentiated and failed to reach the level of emplacement of the more evolved magmas, or that magmas of intermediate composition have been generated by crustal melting. Initial Sr-isotope ratios [$\varepsilon_{Sr}(T) = +30$ to $+58$; Vachette et al. 1968; Ataman 1972] do not help resolve these alternatives since such isotopic ratios are consistent either with a source in the lithospheric mantle, enriched by subduction, or with anatexis of a crustal protolith of intermediate composition.

Fractional crystallisation of basic melts

The geochemical characteristics of the Orhaneli and Topuk granodiorites are consistent with fractionation from a basic melt, as can be seen by comparing their trace-element geochemistry with Basin-and-Range dacites that result from fractional crystallisation of basaltic melts (Davis et al. 1993) or with post-collision Alpine intrusives, such as the quartz diorite-tonalite-granodiorite suite, from Adamello (Dupuy et al. 1982) that are derived largely by fractional crystallisation of a hydrous basalt at pressures of 8–10 kbars (Blundy and Sparks 1992). Intermediate magmas from all three provinces are characterised by enrichment of LIL/HFS element ratios, a lack of depletion in Y and HREE (Figs. 3b, 4b) and $^{87}Sr/^{86}Sr > 0.7065$. Ba abundances, which are markedly higher in the Basin-and-Range dacites than in either the Adamello or the northwest Anatolian intrusives, probably result from the relative stability of phases with a large partition coefficient for Ba, such as phlogopite, in the source regions of the parental magmas.

Studies of subduction-related felsic magmatism ($SiO_2 = 56$ to 73 wt%) have confirmed that melts from a garnet-bearing source are strongly depleted in HREE (Y < 15 ppm, Yb < 1.4; Drummond and Defant 1990). The Orhaneli and Topuk granodiorites are insufficiently depleted in Y (17–25 ppm) and Yb (1.8–4.6 ppm) to have equilibrated with a garnet-bearing restite. Moreover if the granodiorites result from fractional crytallisation from a less evolved magma represented by the dioritic enclaves, Y abudances in the unfractionated magma must have exceeded 40 ppm (Table 2). This suggests that the melt from which the granodiorites are derived formed in the absence of garnet in the restite, and hence resulted from melting of the mantle wedge rather than of the subducted slab.

It is clear that plagioclase crystallisation became important during the formation of the more siliceous magmas in the Topuk intrusion which are characterised by significant negative Eu anomalies (Fig. 4a). This indicates intra-crustal fractionation occurred, within the stability field of plagioclase. The absence of appreciable Eu anomalies in the Orhaneli granodiorite does not preclude an origin from fractional crystallisation of more primitive melts. Geochemical trends from post-subduction calc-alkaline lavas from the Basin-and-Range Province demonstrate that fractionation is dominated by olivine and pyroxene in the early stages ($SiO_2 < 63\%$) and plagioclase fractionation only becomes significant in the generation of more evolved magmas (Davis and Hawkesworth 1993). Eu anomalies are also impeded by high f_{O_2} during fractional crystallisation.

Partial melting of the crust

In contrast to the Adamello suite, cosanguineous gabbros, lamprophyric dykes or basic enclaves have not been found associated with the Orhaneli and Topuk granodiorites. This makes an origin by fractional crystallisation of mantle-derived melts more equivocal. Magmas of intermediate composition can be derived from anatexis of the lower crust by vapour-absent dehydration reactions of biotite and/or amphibole at temperatures between 825° C and 1100° C (Rutter and Wyllie 1988). The biotite dehydration reaction in assemblages of intermediate compositions is given by

$$\text{Biotite} + \text{Quartz} + \text{Plagioclase} = \text{Pyroxene} \pm \text{Garnet} + \text{Melt} \quad (1)$$

yielding a melt of granodioritic composition, and at higher temperatures the incongruent melting of hornblende yields a tonalitic melt through the reaction

$$\text{Hornblende} + \text{Plagioclase} + \text{Quartz} = \text{Pyroxene} \pm \text{Garnet} + \text{Melt} \quad (2)$$

The presence of garnet in the restite, which controls the behaviour of HREE and Y in the melt, is favoured by higher pressures and also by a high Fe/Mg ratio in the source.

Granodiorite from the Idaho batholith provides an example of a melt, with similar major-element composition to the Anatolian intrusives, that has been derived from partial melting of the lower crust in the stability field of garnet (Clarke 1990). Although sharing many of the geochemical trends of the Orhaneli and Topuk granodiorites, it is clearly more depleted in Y and HREE (Figs. 3b, 4b). Thus although the modal composition of a crustal source can not precisely be identified, the absence of HREE depletion indicates that garnet was not a significant restite phase. This has implications for the depths of crustal melting.

Experimental studies of vapour-absent melting of biotite and hornblende indicate that for a tonalitic source, garnet will be stable at pressures of 10 kbar (Rutter and Wyllie 1988) whereas for a source of greywacke composition garnet may be stable on the solidus at pressures as low as 8 kbar (Vielzeuf and Montel 1992). A more basic, amphibolitic source will yield a tonalitic melt through reaction (2) with garnet stable at pressures > 8 kbar (Rushmer 1991).

The temperature of the source is clearly hotter than minimum emplacement temperatures for the magma

(770° C) and may be inferred from the critical melt fraction (Wickham 1987). For $F > 0.3$, sufficient to allow melt extraction through buoyancy, and assuming a tonalitic source, then a temperature of at least 950° C is required at pressures around 10 kbar (Rutter and Wyllie 1988).

Thermal implications

The Orhaneli and Topuk granodiorites have therefore formed either from differentiation of basic magmas in crustal magma chambers, probably at depths of 8–10 kbar, or from the melting of a crustal source at pressures less than 10 kbar. Since we can not conclusively distinguish these petrogeneses on the basis of geochemistry, it is germane to consider whether crustal melting could have occured by purely tectonic processes, in the absence of mantle melting.

Temperatures in excess of 950° C at depths of about 50 km could not have resulted solely from thermal relaxation after tectonic thickening, even if uplift was delayed by tens of millions of years after collision (England and Thompson 1984). Moreover the preservation of blueschist-facies assemblages make it unlikely that conductive heating played a significant role in melting a crustal source region of the granodiorite magma.

Decompression of rocks from depths of around 10 kbar, under vapour-absent conditions, will certainly increase the available melt fraction, provided rocks are close their solidus temperatures prior to uplift. Since the melt fraction available depends on the pressure, temperature and water content of the source it is possible to estimate the maximum melt fraction that can be obtained during decompression. For example the melt fractions obtained for a source of intermediate composition and variable H_2O contents are known for pressures of 5 and 10 kbar (Clemens and Vielzeuf 1987, Fig. 5). If we assume that the source rock has a water content of 0.8%, uplift from 10 kbar (at 950° C) to 5 kbar will result in an increased melt fraction of 0.07. This is a maximum value, since it assumes firstly that melt kinetics will be sufficiently rapid to maintain thermodynamic equilibrium during exhumation and secondly that uplift is sufficiently rapid for the protolith to follow its adiabatic path during exhumation (a slower rate of exhumation will result in loss of heat through conduction and a reduced melt fraction). We do not know precisely either the temperature or the depth of the source, but given that melting was initiated at pressures less than 10 kbar and the magma was emplaced at $\sim$ 3 kbar we can say that the increase in melt fraction obtained by decompression melting of the crust did not exceed 0.1. Such a low melt fraction could not have left its source through buoyancy (Wickham 1987).

The available Ar chronology also does not support decompression melting since there is a lapse of at least 25 Ma (from 88 to 53 Ma) between blueschist-facies metamorphism and intrusion of the granodiorite. Exhumation of the blueschists either occured almost immediately after blueschist-facies metamorphism, or was already underway at the time peak temperatures were recorded. Otherwise, conductive heating in a thickened crust would have resulted in greenschist overprinting of the high P-low T assemblages. Therefore melt formation must have occurred considerably later than exhumation from deep crustal levels. We conclude that melting of a crustal source was caused by heating rather than by decompression.

Thus thermal constraints require that if the plutons are derived from a crustal source, advective heating from mantle-derived melts is required. In other words mantle melting is essential for the petrogenesis of the granodiorites, either to provide a parental magma, as in the case of the Adamello intrusives, or to provide an advective heat source for crustal melting. Evidence for more mafic material associated with intermediate magmatism is restricted to small quartz-diorite enclaves in the granodiorite. Their finer grain size argues against an autolith origin, and is consistent with an origin from a coeval melt.

Regional tectonics and post-collision magmatism

The available sources for post-collision magmatism vary according to both the geometry of the collision zone and the time elapsed between collision and magmatism. Advective heating from mantle-derived melts, as observed in the Adamello Massif, occurs over a time-scale of < 1 Ma (Huppert and Sparks 1988) whereas conductive heating, as observed in the Himalayan orogen, requires a time-scale > 10 Ma (England and Thompson 1984). The spatial and chronological relationships between subduction, collision, and melting in northwest Anatolia are therefore significant.

Final collision between the Tavşanli and Sakarya zones must post-date ophiolite obduction in the region. This is constrained by the Ar-isotope age from the garnet amphibolite of 101.1 ± 3.8 Ma (Fig. 5e) which provides the best available estimate for the age of obduction of the ophiolite onto the continental margin, though strictly it represents a maximum constraint because the late thrusts, which place the ophiolite in its present position, are brittle. The emplacement ages of the northwest Anatolian intrusives ($\sim$ 50 Ma) are some 50 Ma younger than ophiolite obduction, but similar to deposition ages of Mid-Eocene neritic limestones that unconformably overlie the ultramafic rocks above the blueschists, thus suggesting that magmatism occurred within a few million years of collision.

Since the granodiorites were emplaced at a depth of $\sim$ 10 km into blueschist lithologies that had equilibrated at depths of $\sim$ 70 km, about 60 km of uplift occurred between blueschist metamorphism and granodiorite

emplacement. If we take the former at 88 Ma, as determined by Okay and Kelley (1994) and the latter at 53 Ma (Table 3), this suggests a minimum exhumation rate of nearly 2 mm a^{-1} before emplacement of the granodiorites. Conductive-heating models of a simple thrust system suggest that rocks exhumed from depths of 70 km and temperatures of 430° C would undergo significant heating during uplift due to radioactive heat production (England and Thompson 1984). High exhumation rates would result in relatively low maximum temperatures, but because of thermal inertia these would be reached at low pressures. The preservation of high *P*-low *T* assemblages and absence of a regional greenschist overprint in the western part of the Tavşanli Zone blueschists suggest that exhumation did not result simply from isostatic uplift of tectonically thickened crust.

Blueschist-facies assemblages may be exhumed under constant temperature conditions provided that subduction continues during their exhumation. For example, high *P*-low *T* assemblages may be preserved within an imbricated accretionary prism as a consequence of underthrusting by cold material during uplift (Platt 1993). However in the Tavşanli blueschists, lithologies are indicative of a passive continental margin rather than an accretionary prism (Okay 1984). Two-dimensional thermal modelling of subducted continental lithosphere suggests that low maximum temperatures during exhumation may be obtained from delamination of blueschist-facies lithologies of the downgoing slab, followed by buoyancy-driven ascent (Wijbrans et al. 1993). The preservation of blueschist-facies assemblages requires that exhumation takes place within ~ 10 kilometres of an active subduction zone, and the minimum exhumation rate required is 1.5 mm a^{-1} similar to that deduced from the present study of the Tavşanli blueschists. In this model, greenschist overprinting will only be associated with younger isotopic ages and relatively slow uplift rates.

Syn-subduction exhumation also provides an explanation for the possible range of blueschist metamorphic ages (~ 20 Ma). Younger ages, which cover a similar range (42–29 Ma) and have been ascribed to differential uplift and cooling during active subduction, have been obtained from single-grain argon laserprobe analyses of phengites from blueschist-facies assemblages of Sifnos (Greece) (Wijbrans et al. 1990, 1993). These studies predict that younger blueschist-facies ages will be located close to the point of extensional detachment, which in the case of the Tavşanli Zone, is the reactivated thrust between blueschists and ophiolite fragments. At present this model can not be tested in northwest Anatolia since there are only two ages available for blueschist-facies metamorphism from the Tavşanli Zone, both from samples lying within 2 km of the extensional detachment.

The precise geometry of Eocene convergence between the Tavşanli and Sakarya zones is equivocal. A reversal from northwards to southwards subduction of oceanic lithosphere along the Izmir-Ankara suture, as suggested by Sengör et al. (1984), would explain melt generation in the hanging wall of the reversed subduction zone. Alternatively, a second northward-dipping subduction zone may have been initiated south of the Tavşanli Zone. Magmatism occurred during the period immediately following collision in a tectonic setting similar to that of the Adamello Massif. Interestingly both provinces are characterised by an apparent absence of syn-subduction magmatism. Numerical models for *P-T-t* paths at subduction zones indicate that subduction results in cooling the mantle wedge, unless induced convection occurs at shallow depths (< 100 km), in which case melting can occur from the incongruent melting of hornblende (Peacock 1991). In the absence of such convection, cessation of subduction can cause heating in the hanging wall of the hydrated mantle wedge which could trigger melting. The magmas formed beneath the Tavşanli Zone were either modified by fractional crystallisation and possible assimilation during ascent through thickened crust, or triggered crustal melting at pressures less than 10 kbar.

The Orhaneli and Topuk granodiorites are therefore derived from similar source regions as magmas of intermediate composition formed at active continental margins. This study suggests that during the early stages of post-collision tectonics, the sites of melt zones are determined by the thermal structure of the mantle wedge and consequent advective heating of the crust, rather than by thermal conduction in tectonically thickened crust.

Acknowledgements Financial support for this study was provided by NATO Collaborative Research Grant 900412 and by TUBITAK grant TBAG 994/YBAG 0020-Glotek (AIO). Dr Graham Chinner at the Department of Earth Sciences, University of Cambridge is thanked for facilitating the use of the microprobe, Simon Turner for helpful comments and assistance with Ar analyses and Malcolm Hole for a constructive review.

References

Ataman G (1972) Radiometric age of the granodiorite massif of Orhaneli. Turk Jeol Kurumu Bül 15:125–130

Ataman G (1973) Radiometric age of the granodiorite massif of Gürgenyayla. Turk Jeol Kurumu Bül 16:22–26

Bingöl E, Delaloye M, Ataman G (1982) Granitic intrusions in western Anatolia: a contribution of the geodynamic study of this area. Ecol Geol Helv 75:437–446

Blundy JD, Holland TJB (1990) Calcic amphibole equilibria and a new amphibole-plagioclase geothermometer. Contrib Mineral Petrol 104:208–224

Blundy JD, Sparks RSJ (1992) Petrogenesis of mafic inclusions in granitoids of the Adamello Massif, Italy. J Petrol 33:1039–1104

Clarke CB (1990) The geochemistry of the Atlanta lobe of the Idaho batholith in the Western United States (unpublished) PhD thesis, Open Univ, UK

Clemens JD, Vielzeuf D (1987) Constraints on melting and magma production in the crust. Earth Planet Sci Lett 86:287–306

Çoğulu E, Krummenacher D (1967) Problèmes geochronometriques dans la partie NW de l'Anatolie Centrale (Turquie). Schweiz Mineral Petrogr Mitt 47:825–833

Davis J, Hawkesworth CJ (1993) Early calc-alkaline magmatism in the Mogollon-Datil volcanic field, New Mexico, USA. Contrib Mineral Petrol 115:165–183

Davis JM, Elston WE, Hawkesworth CJ (1993) Basic and intermediate volcanism of the Mogollon Datil Volcanic Field: implications for mid-Tertiary tectonic transitions in southwestern New Mexico, USA. In: Pritchard HM, Harris NBW, Alabaster T, Neary CJ (eds) Magmatic processes and plate tectonics. Geol Soc London Spec Publ 76:469–488

De Yoreo JJ, Lux DR, Guidotti CV (1989) The role of crustal anatexis and magma migration in the thermal evolution of regions of thickened continental crust. In: Daly JS, Cliff RA, Yardley BWD (eds) Evolution of metamorphic belts. Geol Soc London Spec Publ 43:187–202

Drummond MS, Defant MJ (1990) A model for trondhjemite-tonalite-dacite genesis and crustal growth via slab melting: Archean to modern comparisons. J Geophys Res 95:21503–21521

Dupuy C, Dostal J, Fratta M (1982) Geochemistry of the Adamello Massif (Northern Italy). Contrib Mineral Petrol 80:41–48

Eaton GP (1982) The Basin and Range Province: origin and tectonic setting. Ann Rev Earth Sci 10:409–440

England PC, Thompson AB (1984) Pressure-temperature-time paths of regional metamorphism. 1. Heat transfer during the evolution of regions of thickened crust. J Petrol 25:894–928

England P, Le Fort P, Molnar P, Pêcher A (1992) Heat sources for Tertiary magmatism and anatexis in the Annapurna-Manaslu region of Central Nepal. J Geophys Res 97:2107–2128

Ercan T, Türkecan A (1984) A general review of the plutons in Western Anatolia, Aegean Islands, Greece and Bulgaria. Ketin Simp, pp 189–208

Hammarstrom JM, Zen E-An (1986) Aluminium in hornblende: an empirical igneous geobarometer. Am Mineral 71:1297–1313

Harris NBW, Massey JA (1994) Decompression and anatexis of Himalayan metapelites. Tectonics (in press)

Hawkesworth CJ, Gallagher K, Kelley S, Mantovani M, Peate DW, Regelous M, Rogers NW (1992) Paraná magmatism and the opening of the South Atlantic. In: Storey BC, Alabaster T, Pankhurst RJ (eds) Magmatism and causes of continental break-up. Geol Soc London Spec Publ 68:221–240

Holland TJB, Powell R (1985) An internally consistent thermodynamic dataset with uncertainties and correlations. 2. Data and results. J Metamorphic Geol 3:343–370

Holland TJB, Powell R (1990) An enlarged and updated internally consistent thermodynamic dataset with uncertainties and correlations: the system K_2O-Na_2O-CaO-MgO-MnO-FeO-Fe_2O_3-Al_2O_3-TiO_2-SiO_2-C-H_2-O_2. J Metamorphic Geol 8:89–124

Houseman GA, McKenzie DP, Molnar P (1981) Convective instability of a thickened boundary layer and its relevance for the thermal evolution of continental convergent belts. J Geophys Res 86:6115–6135

Huppert HE, Sparks RSJ (1988) The generation of granitic magmas by intrusion of basalt into continental crust. J Petrol 29:599–624

Le Breton N, Thompson AB (1988) Fluid-absent (dehydration) melting of biotite in metapelites in the early stages of crustal anatexis. Contrib Mineral Petrol 99:226–237

Lisenbee AL (1972) Structural setting of the Orhaneli ultramafic massif near Bursa, northwestern Turkey (unpublished). PhD thesis, Pennsylvania Univ, USA

Massone H-J, Schreyer W (1987) Phengite geobarometry based on the limiting assemblage with K-feldspar, phlogopite and quartz. Contrib Mineral Petrol 96:212–224

McDowell FW, Lehman DH, Gucwa PR, Fritz D, Maxwell JC (1984) Glaucophane schists and ophiolites of the northern California Coast Ranges: isotopic ages and their tectonic implications. Geol Soc Am Bull 95:1373–1382

Okay AI (1984) Distribution and characteristics of the northwest Turkish blueschists. Geol Soc London Spec Publ 17:455–466

Okay AI (1986) High-pressure/low-temperature metamorphic rocks of Turkey. Geol Soc Am Mem 164:333–347

Okay AI (1989) Alpine-Himalayan blueschists. Ann Rev Earth Planet Sci 17:55–87

Okay AI, Kelley SP (1994) Jadeite and chloritoid schists from northwest Turkey: tectonic setting, petrology and geochronology. J Metamorphic Geol (in press)

Peacock SM (1991) Numerical simulation of subduction zone pressure-temperature-time paths: constraints on fluid production and arc magmatism. Philos Trans R Soc London 335:341–353

Pearce JA, Harris NBW, Tindle AG (1984) Trace-element discrimination diagrams for the tectonic interpretation of granitic rocks. J Petrol 25:956–983

Piwinskii AJ (1973) Experimental studies of granitoids from the Central and Southern Coast Ranges, California. Tschermaks Mineral Petrogr Mitt 20:107–130

Platt JP (1987) The uplift of high pressure-low temperature metamorphic rocks. Phil Trans R Soc London 321:87–103

Platt JP (1993) Exhumation of high-pressure rocks: a review of concepts and processes. Terra Nova 5:119–133

Potts PJ, Thorpe OW, Watson JS (1981) Determination of the REE abundances in 29 international rock standards by Instrumental Neutron Activation: a critical appraisal of calibration errors. Chem Geol 34:331–352

Powell R, Holland TJB (1985) An internally consistent thermodynamic dataset with uncertainties and correlations. 1. methods and a worked example. J Metamorphic Geol 3:327–342

Rushmer T (1991) Partial melting of two amphibolites: contrasting experimental results under fluid-absent conditions. Contrib Mineral Petrol 107:41–59

Rutter MJ, Wyllie PJ (1988) Melting of vapour-absent tonalite at 10 kbar to simulate dehydration melting in the deep crust. Nature 331:159–160

Samson SD, Alexander EC Jr (1987) Calibration of the interlaboratory $^{40}Ar/^{39}Ar$ dating standard, MMhb-1. Chem Geol Isot Geosci Sect 66:27–34

Sandiford MS, Foden J, Shaohua Zhou, Turner S (1992) Granite genesis and the mechanics of convergent orogenic belts with application to the southern Adelaide Fold Belt. Trans R Soc Edinburgh 83:83–93

Schmidt MW (1992) Amphibole composition in tonalite as a function of pressure: an experimental calibration of the Al-in-hornblende-thermometer. Contrib Mineral Petrol 110:304–310

Sengör AMC, Satir M, Akkök R (1984) Timing of tectonic events in the Menderes Massif, Western Turkey: implications for tectonic evolution and evidence for Pan -African basement in Turkey. Tectonics 3:693–707

Sisson VB, Onstott TC (1986) Dating blueschist metamorphism: a combined $^{40}Ar/^{39}Ar$ and electron microprobe approach. Geochim Cosmochim Acta 50:2111–2117

Turner S, Hawkesworth C, Jiaqi Liu, Rogers N, Kelley S, Van Calsteren P (1993) Volcanism on the Tibetan Plateau as an independent constraint on timing of uplift. Nature 364:50–54

Vachette M, Blanc P, Dubertret L (1968) Détermination de l'âge d'une granodiorite d'Orhaneli au Sud de Bursa (Anatolie); sa signification régionale. C R Acad Sci Paris 267:927–930

Vielzeuf D, Montel JM (1992) Experimental determination of fluid-absent melting of a natural quartz-rich metagreywacke. 1. Phase relations. Terra Abstr 3:30

Wickham S (1987) Crustal anatexis and granite petrogenesis during low pressure regional metamorphism: the Trois Seigneurs Massif, Pyrenees, France, J Petrol 28:127–169

Wijbrans JR, Schliestedt M, York D (1990) Single grain argon laser probe dating of phengites from the blueschist to greenschist transition on Sifnos (Greece). Contrib Mineral Petrol 104:582–593

Wijbrans JR, van Wees JD, Stephenson RA, Cloetingh SAPL (1993) Pressure-temperature-time evolution of the high-pressure metamorphic complex of Sifnos, Greece. Geol 21:443–446